Article

Journal of the Brazilian Chemical Society

https://dx.doi.org/10.21577/0103-5053.20240175

*J. Braz. Chem. Soc.* **2025**, *36*, 4, e-20240175, 1-9


# Extraction Mechanism of Hesperidin from *Citrus aurantium* L. Using a Novel Deep Eutectic Solvent: Experimental and Theoretical Investigation

***Jun Zhou*** *** [a] and Jinbao Tang*** [a]

[a]*College of Chemistry and Chemical Engineering, Central South University of Forestry and Technology, 410004 Changsha, P. R. China*

In order to extract hesperidin from *Citrus aurantium* L. through green and efficient ways, a novel method based on deep eutectic solvent (DES) assisted extraction has been developed. Compared to known alkali extraction and acid precipitation or organic solvent (ethanol, methanol) extraction, this new DES system of choline chloride/diethanolamine (DES-14) method exhibited excellent extraction efficiency for hesperidin. Under optimal conditions, the extraction yield of hesperidin reached 6.26 ± 0.05%. Further studies with infrared spectroscopy, $^1$H nuclear magnetic resonance, and density functional theory showed the DES-14 was formed mainly through the interaction of H-bond and van der Waals forces. In addition, scanning electron microscopy and density functional theory revealed the strong dissolving capacity, and the H-bond formation between DES-14 and hesperidin, as well as van der Waals forces all contributed to efficient extraction of hesperidin. The results provide a new strategy for efficient extraction and utilization of hesperidin in *Citrus*.

**Keywords:** *Citrus aurantium* L., hesperidin, deep eutectic solvent, extraction, density functional theory, mechanism

## Introduction

Hesperidin (Hep, 3',5,7-trihydroxy-4'-methoxy-flavanone-7-*O*-rutinoside), is a flavanone glycoside abundantly present in *Citrus* fruits, such as *Citrus limon* (L.) Burm.f., *Citrus reticulata* Blanco, *Citrus aurantium* L. (CAL), etc.[1-3] Hep has demonstrated various potential positive effects, including antioxidant, anti-inflammatory, antibacterial, anti-depressive, and protective effects on the cardiovascular and gastrointestinal systems.[4-6] In addition, Hep has also been proposed to have potential anti-coronavirus disease (COVID-19) properties.[7] Owing to its positive effects, Hep is extensively utilized in the fields of food, medicine, and cosmetics. CAL was confirmed to have a higher content of Hep, which refers to the dried young fruit of limes and cultivated varieties or sweet oranges from the genus *Citrus* (family Rutaceae).[8] It has been used as a traditional Chinese medicine for over two thousand years. Modern pharmacological studies have revealed that CAL contains flavonoids, alkaloids, volatile oils, polysaccharides, and a small amount of coumarins, carotenes, riboflavin, and other active ingredients.[9,10] Consequently, Hep has long been the primary target substance for extraction in the *Citrus* extract industry. Currently, Hep is typically extracted using solvent extraction methods (methanol or ethanol),[11,12] alkali extraction and acid precipitation method.[13] However, these methods are associated with limitations such as time-consuming processes, low extraction yields, and negative environmental impacts, which hinder the industry's sustainable and high-quality development. Therefore, the development of green and efficient extraction and separation technologies has emerged as a recent trend. Some of the main technologies that have been explored include mechanochemical-assisted extraction,[14] pressurized hot water extraction,[15] ultrasonic-assisted extraction,[16-18] microwave-assisted extraction,[19] and deep eutectic solvents (DES) extraction,[20] etc. These studies have played a crucial role in advancing the green and efficient extraction and utilization of Hep. Among them, DES extraction has garnered significant attention in the field of plant extracts as a sustainable and environmentally friendly solvent.[21]

DES was originally proposed by Abbott *et al.*[22] in 2003 as a eutectic mixture consisting of a hydrogen bond acceptor (HBA) and a hydrogen bond donor (HBD) in a specific molar ratio. Common HBA compounds including choline chloride (Chcl), betaine, and menthol, while HBD

*e-mail: zhoujun263217@163.com
Editor handled this article: Hector Henrique F. Koolen (Associate)

compounds covering organic acids, amines, alcohols, and amino acids.[23-25] DES exhibit a lower melting point than their individual components, resulting in a strong dissolution ability. Additionally, DES have the advantages of being natural, inexpensive, easily obtainable, simple to prepare, and environmentally friendly. Several DES, such as choline chloride/acetamide, proline/urea, and betaine/ethanol, have been reported for the extraction of Hep,[26-28] leading to the successful extraction of Hep. However, the aforementioned studies are primarily focused on experimental investigations, and limited research available on the screening of novel DES, their formation mechanisms, and the extraction mechanisms of Hep at the molecular level.

In this paper, a novel DES extraction method was developed for extracting Hep from CAL for the first time. A series of Chcl based DESs were prepared and used as extraction solvents to Hep extraction. The crucial parameters of the extraction process were optimized. Afterwards, the formation mechanism of the DES and the potential mechanism of Hep extraction by combining experimental and density functional theory (DFT) calculations were performed. This is the first time that a DES extraction method was successfully developed for Hep extraction from CAL, along with the experimental, and DFT calculations to analyze this phenomenon.

## Experimental

### Chemical reagents

*Citrus aurantium* L. (CAL) was picked in May 2021 from Zhangjiajie Farm (Zhangjiajie, China) and naturally dried. Choline chloride (Chcl, 98%) was purchased of Macklin (Shanghai, China). Acetic acid (Gac, 99.5%), oxalic acid (Oa, 99.8%), lactic acid (La, 85-92%), DL-malic acid (AlMa, 99%), citric acid (Ca, 99.5%), tartaric acid (Ta, 99%), L-lysine (Lly, 98%), glycerol (Gly, 99%), ethyl alcohol (Aea, 99.7%), glucose, maltose (Glu and Mal, 99%), urea (Ure, 99%), ethanolamine (Eta, 99%), diethanolamine (Dia, 98%), triethanolamine (Tra, 85-92%), and methanol (Met, 99.5%) were purchased of Sinopharm Chemical Reagent Co. Ltd. (Shanghai, China) and used in this study. Hep (97%) was purchased of Bailingwei Technology (Beijing, China). All other chemicals were of analytical grade.

### Preparation of the deep eutectic solvent (DES)

Chcl was used as the hydrogen bond acceptor (HBA) and acetic acid, oxalic acid, lactic acid, DL-malic acid, citric acid, tartaric acid, L-lysine, glycerol, ethyl alcohol, glucose, maltose, urea, ethanolamine, diethanolamine, and triethanolamine were used as the hydrogen bond donors (HBD). These components were added to beakers in different molar ratios. The mixture was then magnetically stirred in a constant temperature water bath at 80 °C to promote dissolution. Once a transparent clarified liquid was formed, it was maintained at 40 °C for 4 h. The solution was considered a stable eutectic solvent if no solid precipitation occurred and there were no significant changes in the solution.

### Process and optimization of Hep extraction from CAL by DES

The extraction process was referring to literature concerned.[29] Briefly, the naturally air-dried CAL was crushed using a FW100 high speed crusher (Taisite instrument, Tianjin, China), and less than 40 mesh CAL powders were obtained by sieving. Then, 200 mg powder were taken into 10 mL centrifuge tube, 1.4 mL DES and 0.6 mL water were added and mixed well. Extraction conditions were extraction temperature at 40 °C, vibration speed at 150 rpm, and extraction time for 30 min. Samples were centrifuged (10 000 rpm, 10 min) after extraction. The supernatant was filtered by 0.45 μm filter membrane, and diluted with methanol to be measured by high performance liquid chromatography (HPLC) of Agilent 1260 (Agilent, Santa Clara, United States). The standard curve of Hep was $y = 46\,573\,x + 104.62$, correlation coefficient ($R^2$) = 0.998, the linear relationship was good in the range of 0.02 to 0.10 mg $mL^{-1}$. The analytical column used was as Agilent ZORBAX ODS C-18 (4.6 × 250 mm, 5 μm) at a flow rate of 0.8 mL $min^{-1}$ of methanol and 0.5% acetic acid aqueous solution (45:55, v/v). The column temperature and injection volume were 40 °C and 20 μL, respectively. Extraction rate of Hep was calculated as indicated in equation 1.

$$\text{HEY} / \% = \frac{M_1}{M_2} \times 100 \quad (1)$$

where, HEY is Hep extraction yield in %; $M_1$ is Hep content in the extract in mg; $M_2$ is the weight of CAL powder in mg.

### Properties characterization

Fourier transform infrared (FTIR) spectra were used to analyzed the structure of samples by a Alpha II spectrometer model (Bruker, Billerica, United States). The dried KBr and the sample were pressed into a tablet. The tablet was tested with a scanning wavenumber range of 4000 to 400 $cm^{-1}$, using

32 scanning times at a frequency of 64 Hz. Additionally, the sample was analyzed using a AVANCE NEO $^{1}$H nuclear magnetic resonance (NMR, Bruker, Billerica, United States). The frequency used was 400.15 MHz, the excitation power was set at 24.48 W, the relaxation delay time was 1.00 s, the sampling time was 4.00 s, and the sampling number was 16 t. A JSM-7610FPlus scanning electron microscope (JEOL, Tokyo, Japan) was used to observe the samples of CAL before and after DES extraction. The samples were treated with gold spray and observed at an accelerating voltage of 10 kV.

### DFT calculation

The Gaussian 09 software[30] was utilized for conducting DFT calculations. The 6-31++g (d, p) basis set was employed for the genome level analysis of structural optimization, as well as to investigate the interaction relationship between Chcl and Dia. Additionally, the extraction process of hesperidin by DES-14 was studied using the LC-WPBE level in the DFT calculation.[30] To visualize the interaction mechanism, Multiwfn[31] and VMD[32] software were employed. Moreover, the binding energy of the Chcl and Dia complex was calculated, and the results were corrected using basis set superposition error (BSSE).

$$\Delta E = E_T - \Sigma E_{Chcl} - \Sigma E_{Dia} + \Sigma_{BSSE} \quad (2)$$

where, $E_T$ is the total energy of the complex, $\Sigma E_{Chcl}$ and $\Sigma E_{Dia}$ are the total energy of the Chcl and Dia molecules, respectively. $E_{BSSE}$ is the energy of complex BSSE correction.

## Results and Discussion

### Screening and preparation of DES

In the study of using DES as a solvent to extract natural products, Chcl is a common HBA.[33] Previous studies[34] have shown that Hep exhibits good solubility in Chcl-based DESs. Therefore, we used Chcl as the HBA and adjusted the molar ratio of HBA and HBD, then screen and prepare stable DES by heating and stirring method. 17 kinds of stable DES were obtained and are shown in Table 1, including eight organic acid-based DESs (DES-1 to DES-8), three alcohol-based DESs (DES-9 to DES-11), and six amine-based DESs (DES-12 to DES-17) . In most cases, water plays an important role in regulating the viscosity to improve the extraction effect.[35] Hence, the Hep extraction efficiency was tested for each of 17 different DES - aqueous solution as solvents from CAL.

**Table 1.** The composition of stable DES obtained through screening

| Abbreviation | HBA | HBD | Molar ratio |
|---|---|---|---|
| DES-1 | choline chloride | acetic acid | 1:2 |
| DES-2 | | | 1:3 |
| DES-3 | | oxalic acid | 2:1 |
| DES-4 | | | 1:1 |
| DES-5 | | lactic acid | 1:1 |
| DES-6 | | | 1:2 |
| DES-7 | | | 1:3 |
| DES-8 | | DL-malic acid | 1:1 |
| DES-9 | | glycerol | 1:2 |
| DES-10 | | | 1:3 |
| DES-11 | | ethyl alcohol | 1:8 |
| DES-12 | | urea | 1:2 |
| DES-13 | | ethanolamine | 1:8 |
| DES-14 | | diethanolamine | 1:5 |
| DES-15 | | triethanolamine | 1:1 |
| DES-16 | | | 1:2 |
| DES-17 | | | 1:3 |

HBA: hydrogen bond acceptor; HBD: hydrogen bond donor.

### Hep extraction from CAL with DES

HPLC was used for quantitative analysis of Hep in the extracted samples. Figure 1a demonstrates that Hep exhibits a good separation effect. Seventeen different stable DES, mixed with 30% water, were employed as solvents for the extraction of Hep from CAL. The results are depicted in Figure 1b. It was observed that the extraction efficiency of Hep was higher when Dia was used as the HBD. This might be attributed to the suitable polarity of the extraction solvent. Additionally, we evaluated the main factors influencing the extraction process, including water content, solid-liquid ratio, extraction temperature, and extraction time. As shown in Figure 1c, the extraction yield of Hep initially increased and then decreased with increasing water content in the extraction solvent. The highest yield was achieved at a water content of 40%. This can be attributed to the fact that the addition of water altered the viscosity and solvent polarity, thereby enhancing mass transfer efficiency during the extraction process.[36] However, excessive water caused significant changes in the polarity and pH value of the solvent, which were not favorable for Hep extraction. Figure 1d illustrates the impact of the solid-liquid ratio on extraction yield. When the ratio exceeded 1:12.5 (g mL$^{-1}$), the extraction yield of Hep tended to stabilize. This is due to the larger amount of solvent, which allows for better contact between the solvent and the raw material powder. This results in improved mass transfer and faster diffusion

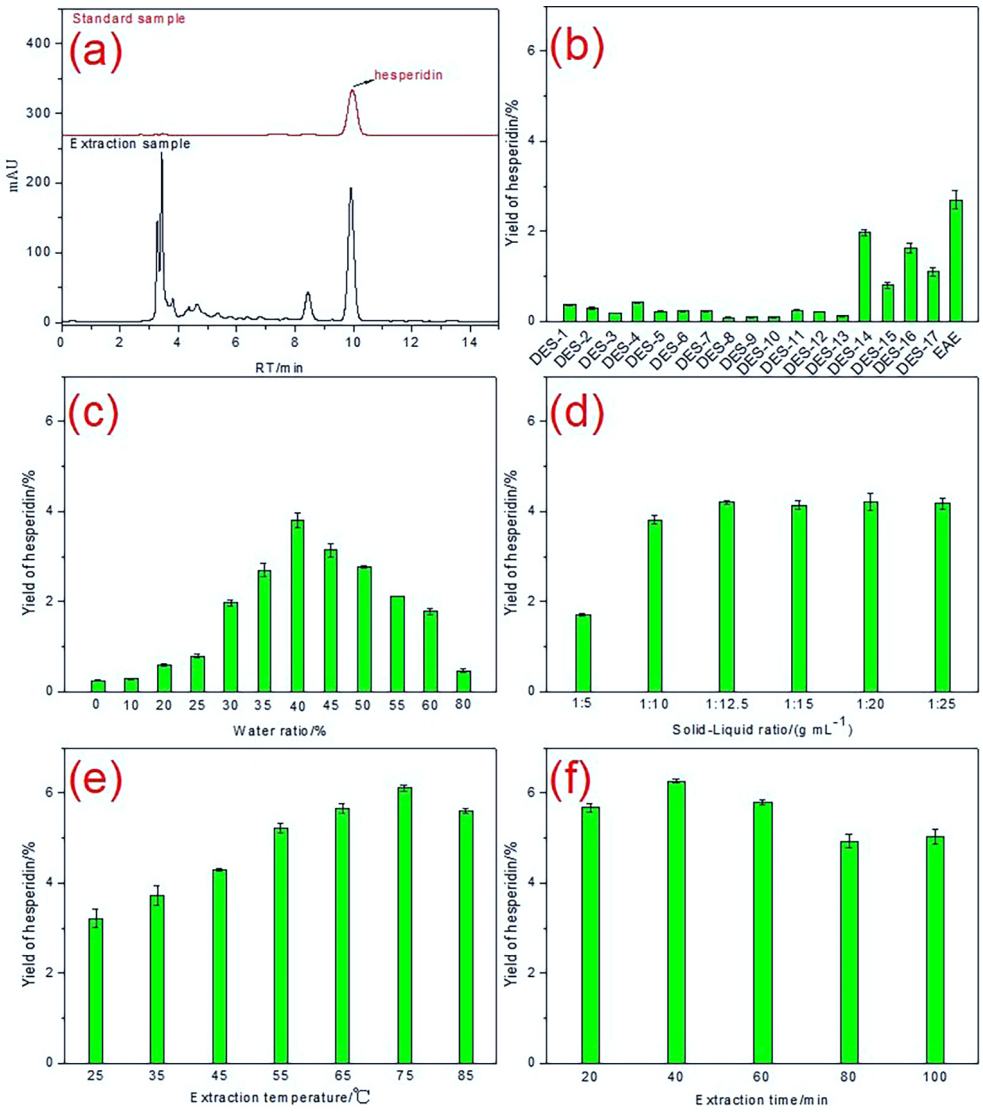


**Figure 1.** Effects of different factors on hesperidin extraction. (a) HPLC analysis of extraction sample. (b) Effects of different DES systems on hesperidin extraction. (c) Effects of different water content on hesperidin extraction. (d) Effects of solid-liquid ratio on hesperidin extraction. (e) Effects of extraction time on hesperidin extraction. (f) Effects of extraction temperature on hesperidin extraction.

rates. The effect of extraction temperature on the extraction yield is shown in Figure 1e. As the extraction temperature increases, the extraction yield initially increases and then decreases, reaching its maximum at 75 °C. This could be attributed to the fact that higher temperatures improve the fluidity of the solvent and accelerate thermal movement between molecules. This leads to increased dissolution and diffusion capacity of the solvent, facilitating mass transfer. However, excessively high temperatures may reduce the stability of Hep. Finally, the effect of extraction time on Hep extraction yield was investigated, and the results are shown in Figure 1f. The extraction yield was highest when the extraction time was 40 min, and it slightly decreased with prolonged extraction time. This can be attributed to the saturation of Hep dissolution during the extraction process, approaching complete extraction. However, the stability of Hep decreased after long extraction at higher temperatures. Therefore, using DES-14 with 40% water content as the extraction solvent, a solid-liquid ratio of 1:12.5 (g $mL^{-1}$), an extraction temperature of 75 °C, and an extraction time of 40 min, the yield of Hep was found to be 6.26 ± 0.05%. This extraction yield was significantly higher than that obtained by using 70% ethanol extraction, as well as alkali extraction and acid precipitation methods.[13]

## Mechanism of DES formation

The formation mechanism of DES-14 was studied through FTIR and $^1$H NMR analysis. In the FTIR (KBr) analysis depicted in Figure 2a, the vibrations corresponding to C–N, C–O, and O–H in Chcl and Dia were identified at 1056, 1402, and 3386 $cm^{-1}$, respectively.[37] These

characteristic functional groups were also observed in DES-14. Furthermore, the vibration of the characteristic absorption peak of DES-14 in the range of 2800 to 3060 $cm^{-1}$ was significantly enhanced, resulting in a strong and broad absorption peak. This suggests that a robust OH···O bond and OH···N bond were formed between Chcl and Dia. $^1$H NMR (DMSO-$d_6$) analysis in Figure 2b showed that during the format of DES-14, the H peaks formed by Chcl and Dia were still present in proportion in DES-14, indicating that no chemical reaction occurred during the formation of DES-14, and there was no chemical bond breakage or structural change. However, the H atom on –OH in the region between the red dashed lines showed a certain chemical shift, indicating that a new hydrogen bond was formed in DES-14, which altered the chemical environment of the H atom and resulted in a change in chemical shift.[38]

Next, we performed optimization of the molecular structures of Chcl and Dia and conducted reduced density gradient (RDG) analysis using DFT calculation. RDG analysis is an important tool for investigating weak interactions such as H-bonding and van der Waals forces, as it provides insight into the intensity of charge distribution.[39] As shown in Figure 3, the atom of O and N exhibited negative charge intensity, while the surrounding H atoms were positive. The methyl and methylene groups were mostly neutral. In the case of Dia, strong negative charge intensity was observed around the O and N atoms, while the vicinity of the H atoms with –NH and –OH groups exhibited positive charge intensity. Therefore, in the formation of DES-14, the positive and negative charge intensity of Chcl and Dia should attract each other, providing a theoretical basis for further structural optimization.

Based on the above results, we performed an optimized conformation of possible H-bond between Chcl and Dia by DFT calculation, and the results are shown in Figure 4. Figure 4Aa displays a strong H-bond at O19–H26···N3 (1.82 Å), which is a much shorter distance than the van der Waals interaction. The –N– is from the Dia molecule acting as the HBD, while the –OH group from the Chcl molecule acts as the HBA. Figure 4Ab shows that the H-bond is formed at O19–H12···N3 (2.35 Å). Figure 4Ac forms hydrogen bonds at O1–H17···O19 (1.95 Å), and Figure 4Ad forms a strong hydrogen bond at O19–H26···O1 (1.83 Å). It should be noted that the dotted lines here represent only distances shorter than the van der Waals interaction radius and do not represent the internal interactions of Chcl or Dia. Based on the length of the hydrogen bonds, the stability order can be roughly determined as: (a) > (d) > (c) > (b).

The binding energies of different conformations were calculated using equation 2, and the results are presented in Table 2. The calculation results reveal that the thermal stability order of each structure is (d) > (a) > (c) > (b). It should be noted that (d) is slightly more stable than (a), which may be attributed to intra-molecular forces.

The optimization of the geometric structure illustrated that a stable hydrogen bond could be formed between Chcl and Dia, which suggests that the interaction between groups in the mixture might be the primary factor contributing to the decrease in DES melting point. Furthermore, an RDG analysis of intra-molecular forces was conducted. Figure 4B demonstrates the intra-molecular characterization of H-bond, van der Waals forces, and spatial repulsion forces. In this figure, the color blue represents strongly attractive interactions, such as H-bond and halogen bond, while red represents a strong repulsive steric effect.[40] The presence of more steric hindrance makes the formation of DES more challenging. The transitional green area in Figure 4B indicates weak van der Waals forces. Notably, between the monomers of (a) and (d), the predominant color is blue, suggesting

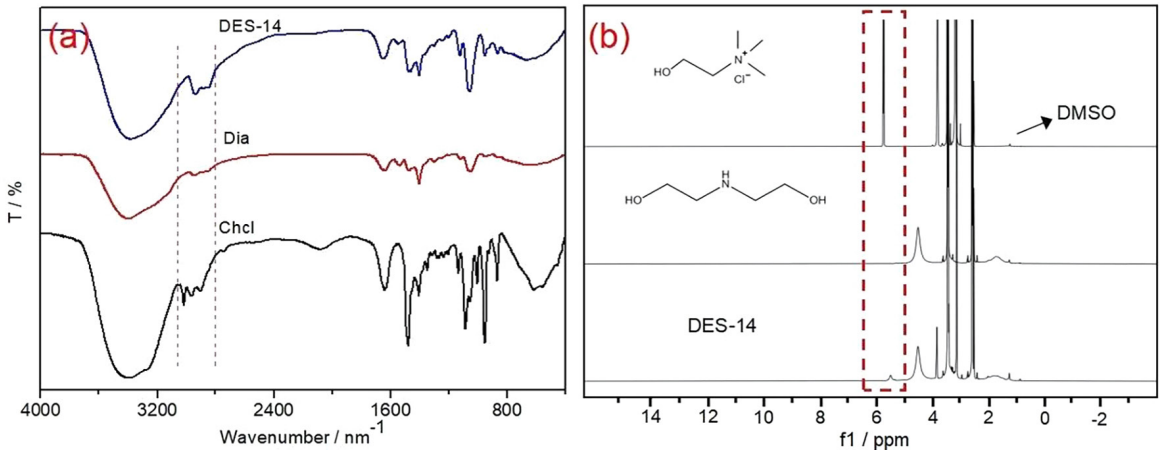


**Figure 2.** (a) FTIR (KBr) and (b) $^1$H NMR (400.15 MHz, DMSO-$d_6$) spectrum of samples.

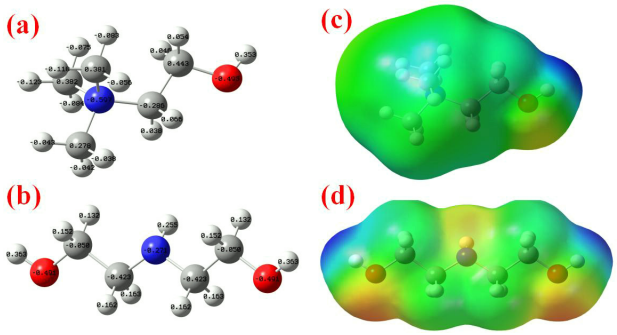


**Figure 3.** Molecular structure optimization (a,b) and RDG analysis (c,d) of Chcl and Dia.

that the H-bond formed by (a) and (d) exhibits strong attraction. Moreover, large green sheets were observed in (a) and (d), indicating the presence of the van der Waals weak force. This suggests that (a) and (d) were relatively stable. On the other hand, (b) and (c) exhibited a green pie, which represents a weak H-bond force. Additionally, their transition green region was small, suggesting a small van der Waals force. As a result, the stability of (b) and (c) was poor. Therefore, in the formation of DES-14, both H-bond and van der Waals forces coexisted, with the H-bond playing a major role. This relationship is associated with the formation and melting point of DES. The stronger the hydrogen bond and van der Waals force, the more stable the structure of DES.

## Extraction mechanism of Hep

After clarifying the formation mechanism of DES-14, the scanning electron microscopy (SEM) analysis was conducted on the appearance of CAL powder before and after DES extraction. As shown in Figure 5a, the cells of the untreated CAL powder were densely packed with a smooth surface. However, after DES-14 extraction, the surface of CAL exhibited obvious damage and numerous folds were observed. This can be attributed to the dissolution of the cell wall by DES-14, leading to the destruction of the cell wall structure.[40] Consequently, the cell permeability increased, resulting in the extravasation of cell fluid and dissolution of the active component in DES-14, thereby enhancing the extraction yield of Hep.

DES has been shown to have the capability to not only disrupt the cell structure, but also enhance the dissolution of the target extract.[21,41] To gain insights into the mechanism of Hep extraction by examining intermolecular forces, we first optimized the geometric structure of Hep and conducted RDG visualization analysis. Figure 6 illustrates that the negative charge intensity in Hep molecules is predominantly situated around the O atoms, with the O atoms in each ring structure exhibiting lower negative charge. Conversely, the O atoms in the –OH group presented a higher degree of negativity, particularly O12,

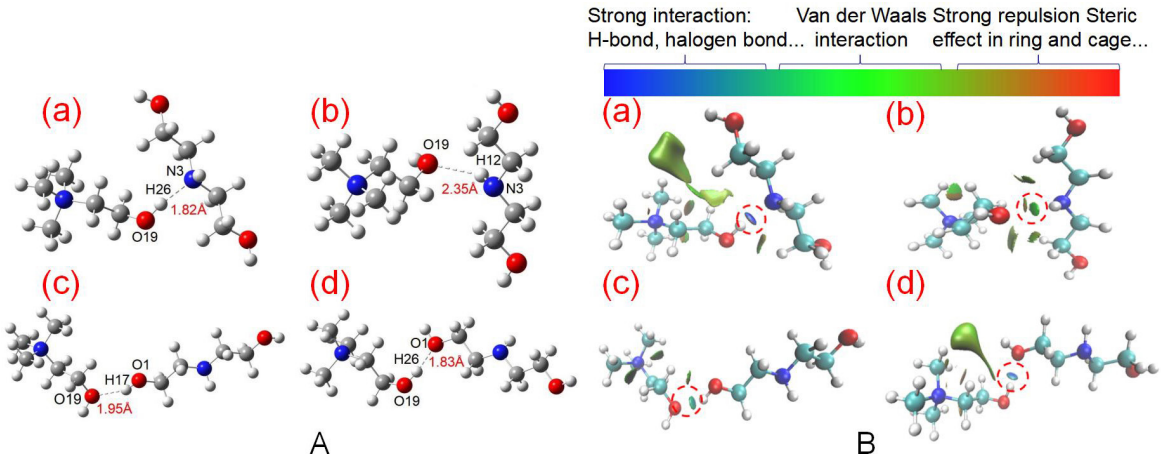


**Figure 4.** Molecular structure optimization (A) and RDG analysis (B) of DES-14.

**Table 2.** The calculation of the binding energy with possible ChCl/Dia structures

| Structure of Chcl/Dia | Total energy of mixture / Hartree | Energy of Chcl / Hartree | Energy of Dia / Hartree | Basis set superposition error | Binding energy / (kcal mol$^{-1}$) |
|---|---|---|---|---|---|
| a | –692.713173 | –328.617834 | –364.082285 | 0.001890 | –28.205436 |
| b | –692.702968 | | | 0.000871 | –4.9969572 |
| c | –692.706726 | | | 0.000941 | –14.314964 |
| d | –692.712767 | | | 0.001395 | –28.431562 |

Chcl: choline chloride; Dia: diethanolamine.

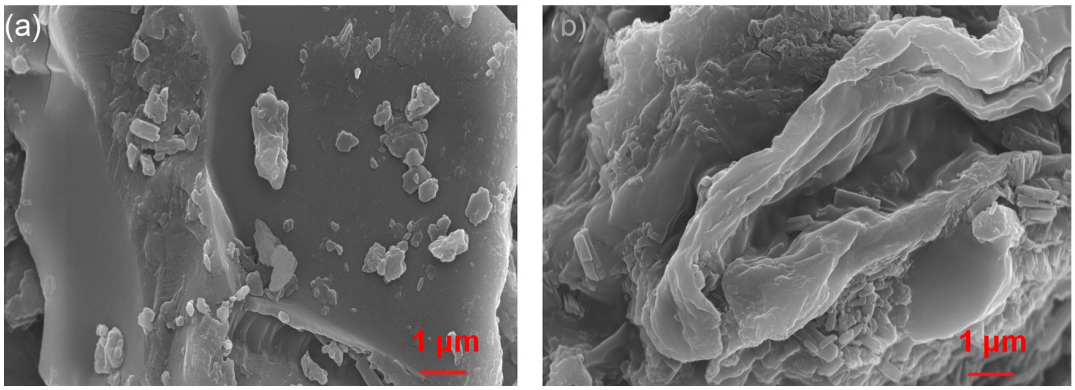


**Figure 5.** SEM of CAL powder before (a) and after (b) extraction by DES-14.

O13, O14, and O15. H atoms possess positive charge, while methyl groups and six-membered rings are neutrally charged. During the extraction process, the positive region of DES-14 interacts with the negative region of the Hep molecule, while the negative region of DES-14 interacts with the positive region of the Hep molecule, resulting in enhanced stability and efficiency.

Based on this, Hep molecules were introduced into DES-14. As shown in Figure 7a, the H-bonds N80–H89···O13 (2.09 Å), O79–H95···O15 (1.98 Å), O15–H74···O96 (2.02 Å), O96–H103···O14 (1.91 Å) were formed. Furthermore, the RDG analysis in Figure 7b demonstrated that H-bonding was the main driving force behind the interaction between DES-14 and Hep molecules, with four H-bonds formed (highlighted by dotted red lines in the figure). In addition to H-bonds, van der Waals forces and other interactions were also present. The red cake represented steric hindrance, primarily observed in Hep molecules, indicating that the repulsion between DES-14 and Hep molecules was minimal. The RDG scatter plot in Figure 7c revealed a blue region indicating clear attraction, such as O96–H103···O14 (1.91Å). The green areas indicate the locations where van der Waals forces or weak hydrogen bonds, such as N80–H89···O13 (2.09 Å), play a role. Additionally, the van der Waals force is present in the green area between them. On the other hand, the red region indicates the presence of steric hindrance, which could be attributed to the existence of significant intra-molecular repulsive forces within Hep itself.

The aforementioned studies have demonstrated that the extraction of Hep by DES-14 resulted in the destruction of the cell structure of CAL. Simultaneously, DES-14, acting as the solvent for extraction, interacted with Hep molecules through H-bonding and van der Waals forces, thereby facilitating the dissolution of Hep. These findings suggest that DES-14 holds potential for the extraction of Hep from CAL.

## Conclusions

In this study, a new DES extraction method was developed and validated for the extraction of Hep from CAL. The DES-14 system, consisting of Chcl as the HBA and Dia as the HBD, was used as the extraction solvent (molar ratio of 1:5). The extraction conditions included 40% water content, a solid/liquid ratio of 1:12.5 (g $mL^{-1}$), an extraction temperature of 75 °C, and an extraction time of 40 min. The extraction yield of Hep obtained under these conditions was 6.26 ± 0.05%. Compared to conventional organic solvent extraction and alkali extraction and acid precipitation method, the DES-14 extraction method demonstrated excellent extraction performance for Hep. Furthermore, the results demonstrated that hydrogen

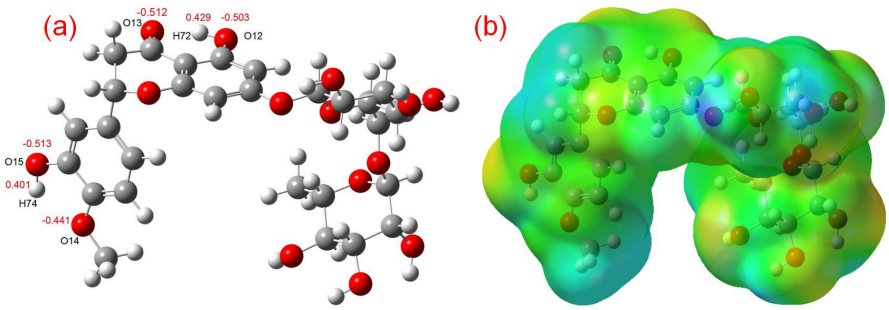


**Figure 6.** Molecular structure optimization (a) and RDG analysis (b) of hesperidin.

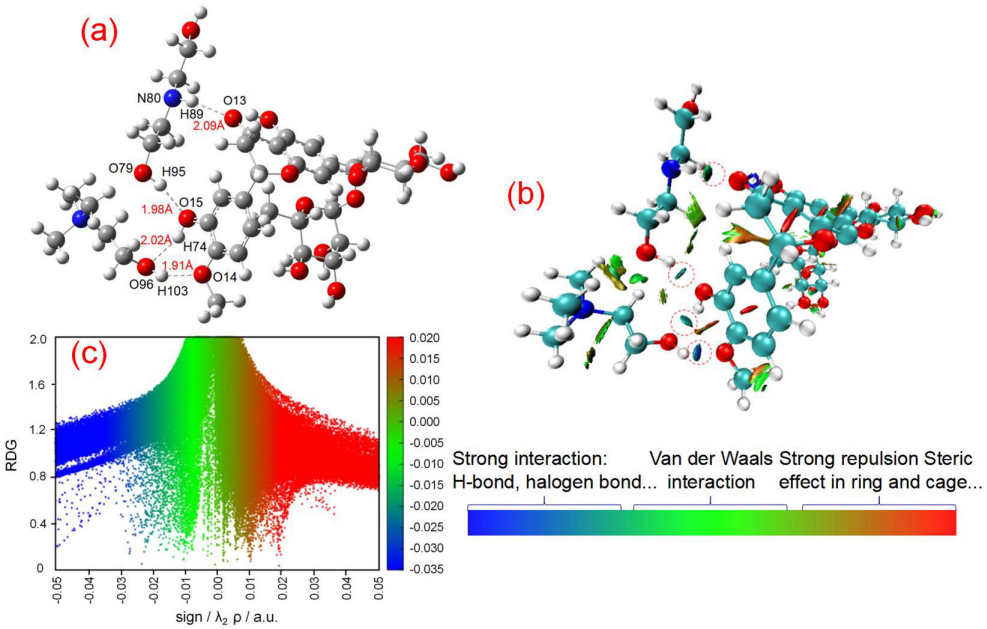


**Figure 7.** Structure optimization (a), RDG analysis (b) and RDG scatter figure (c) of DES-14 and hesperidin in extraction process.

bonding and van der Waals interactions played a crucial role in the formation of DES-14. The excellent extraction capability of DES-14 for hesperidin can be attributed to its high solubility, as well as the strong hydrogen bonding and van der Waals interactions between DES-14 and Hep. This study provides a comprehensive investigation into the extraction efficiency and the underlying mechanism of a novel DES extraction method for Hep, laying the foundation for the future application of DES in the extraction and purification of Hep from *Citrus*.

## Acknowledgments

This work was financially supported by Guangxi Key Laboratory of Chemistry and Engineering of Forest Products (grant No. GXFK2302), the National Key Research and Development Program of China (grant No. 2022YFD2200605), the Postgraduate Science and Technology Innovation Fund of Hunan Province (grant No. CX20230737) and the Postgraduate Science and Technology Innovation Fund of Central South University of Forestry and Technology (grant No. 2023CX01016).

## References

1. Klimek-Szczykutowicz, M.; Szopa, A.; Ekiert H.; *Plants* **2020**, *9*, 119. [Crossref]
2. Kumar, A.; Rout, R. K.; Rao, P. S.; Prabhakar, P.; *J. Food Process Eng.* **2023**, *46*, e14111. [Crossref]
3. Yao, Y.; Lin, M. Y.; Liu, Z. J.; Liu, M. Y.; Zhang, S. H., Zhang, Y. K.; *Front Pharmacol.* **2022**, *13*, 918665. [Crossref]
4. Roohbakhsh, A.; Parhiz, H.; Soltani, F.; Rezaee, R.; Iranshahi, M.; *Life Sci.* **2015**, *124*, 64. [Crossref]
5. Zheng, M.; Lu, S. M.; Xing, J. R.; *Food Chem.* **2021**, *336*, 127539. [Crossref]
6. Pyrzynska, K.; *Nutrients* **2022**, *14*, 2387. [Crossref]
7. Meneguzzo, F.; Ciriminna, R.; Zabini, F.; Pagliaro, M.; *Processes* **2020**, *8*, 549. [Crossref]
8. Yang, L.; Cao, Y.-L.; Jiang, J.-G.; Lin, Q.-S.; Chen, J.; Zhu, L.; *J. Sep. Sci.* **2010**, *33*, 1349. [Crossref]
9. Družić, J.; Jerković, I.; Marijanović, Z.; Roje, M.; *J. Essent. Oil Res*. **2016**, *28*, 283. [Crossref]
10. Xiong, Y.; Chang, M.; Deng, K.; Luo, Y.; *Nat. Prod. Res.* **2016**, *30*, 1571. [Crossref]
11. de la Rosa, J. D. P.; Ruiz-Palomino, P.; Arriola-Guevara, E.; García-Fajardo, J.; Sandoval, G.; Guatemala-Morales, G. M.; *Processes* **2018**, *6*, 266. [Crossref]
12. Phucharoenrak, P.; Muangnoi, C.; T rachootham, D.; *Molecules* **2022**, *27*, 820. [Crossref]
13. Zhou, P.; Zheng, M.; Li, X. Z.; Zhou, J.; Shang, Y. X.; Li, Z. S.; Qu, L. M.; *Ind. Crops Prod.* **2022**, *182*, 114849. [Crossref]
14. Jokić, S.; Molnar, M.; Cikoš, A. M.; Jakovljević, M.; Šafranko, S.; Jerković, I.; *Sep. Sci. Technol.* **2019**, *55*, 2799. [Crossref]
15. Alasalvar, H.; Kaya, M.; Berktas, S.; Basyigit, B.; Cam, M.; *Int. J. Food Sci. Tech.* **2023**, *58*, 2060. [Crossref]
16. Ma, Y. Q.; Ye, X. Q.; Hao, Y. B.; Xu, G. N.; Xu, G. H.; Liu, D. H.; *Ultrason. Sonochem.* **2008**, *15*, 227. [Crossref]
17. Nipornram, S.; Tochampa, W.; Rattanatraiwong, P.; Singanusong, R.; *Food Chem.* **2018**, *241*, 3385. [Crossref]
18. Jin, T. Y.; Yu, M. J.; Cao, M. X.; Zhu, X. Y.; *Food Sci. Technol.* **2022**, *42*, e79821. [Crossref]

19. Inoue, T.; Tsubaki, S.; Ogawa, K.; Onishi, K.; Azuma, J.; *Food Chem.* **2010**, *123*, 542. [Crossref]
20. Bajkacz, S.; Adamek, J.; *Food Anal. Methods* **2017**, *11*, 1330. [Crossref]
21. Deng, W. W.; Mei, X. P.; Cheng, Z. J.; Gan, T. X.; Tian, X.; Hu, J. N.; Zang, C. R.; Sun, B.; Wu, J.; Deng, Y.; Ghiladi, R. A.; Lorimer, G. H.; Keceli, G.; Wang, J.; *Food Chem.* **2023**, *405*, 134817. [Crossref]
22. Abbott, A. P.; Capper, G.; Davies, D. L.; Rasheed, R. K.; Tambyrajah, V.; *Chem. Commun.* **2003**, *1*, 70. [Crossref]
23. Zhang, L. J.; Wang, M. S.; *Int. J. Biol. Macromol.* **2017**, *95*, 675. [Crossref]
24. Das, A. K.; Sharma, M.; Mondal, D.; Prasad, K.; *Carbohydr. Polym.* **2016**, *136*, 930. [Crossref]
25. Liu, Y. H.; Li, J.; Fu, R. X.; Zhang, L. L.; Wang, D. Z.; Wang, S.; *Ind. Crops Prod.* **2019**, *140*, 111620. [Crossref]
26. Jokić, S.; Šafranko, S.; Jakovljević, M.; Cikoš, A. M.; Kajić, N.; Kolarević, F.; Babić, J.; Molnar, M.; *Processes* **2019**, *7*, 469. [Crossref]
27. Li, G.; Lei, J.; Li, S. H.; Jiang, Y. M.; Zhang, F.; Song, C. W.; Xiao, S. J.; Fu, S. B.; Zhou, J.Q.; Wu, F. M.; Wang, G.; *RSC Adv.* **2022**, *12*, 26975. [Crossref]
28. Liu, Y. J.; Zhang, H.; Yu, H. M.; Guo, S. H.; Chen, D. W.; *Phytochem. Anal.* **2018**, *30*, 156. [Crossref]
29. Gu, T. N.; Zhang, M. L.; Tan, T.; Chen, J.; Li, Z.; Zhang, Q. H.; Qiu, H. D.; *Chem. Commum.* **2014**, *50*, 11749. [Crossref]
30. Frisch, M. J.; Trucks, G. W.; Schlegel, H. B.; Scuseria, G. E.; Robb, M. A.; Cheeseman, J. R.; Scalmani, G.; Barone, V.; Mennucci, B.; Petersson, G. A.; Nakatsuji, H.; Caricato, M.; Li, X.; Hratchian, H. P.; Izmaylov, A. F.; Bloino, J.; Zheng, G.; Sonnenberg, J. L.; Hada, M.; Ehara, M.; Toyota, K.; Fukuda, R.; Hasegawa, J.; Ishida, M.; Nakajima, T.; Honda, Y.; Kitao, O.; Nakai, H.; Vreven, T.; Montgomery Jr., J. A.; Peralta, J. E.; Ogliaro, F.; Bearpark, M.; Heyd, J. J.; Brothers, E.; Kudin, K. N.; Staroverov, V. N.; Kobayashi, R.; Normand, J.; Raghavachari, K.; Rendell, A.; Burant, J. C.; Iyengar, S. S.; Tomasi, J.; Cossi, M.; Rega, N.; Millam, N. J.; Klene, M.; Knox, J. E.; Cross, J. B.; Bakken, V.; Adamo, C.; Jaramillo, J.; Gomperts, R.; Stratmann, R. E.; Yazyev, O.; Austin, A. J.; Cammi, R.; Pomelli, C.; Ochterski, J. W.; Martin, R. L.; Morokuma, K.; Zakrzewski, V. G.; Voth, G. A.; Salvador, P.; Dannenberg, J. J.; Dapprich, S.; Daniels, A. D.; Farkas, Ö.; Foresman, J. B.; Ortiz, J. V.; Cioslowski, J.; Fox, D. J.; *Gaussian-09*, Revision D.01; Gaussian, Inc., Wallingford CT, 2009.
31. Lu, T.; *Multiwfn*, 2.1.2; Beijing Kein Research Center for Natural Sciences, China, 2012.
32. Schulten, K.; *VMD*,1.9.4; University of Illinois, Urbana-Champaign, USA, 2020.
33. Chaves, J. O.; de Souza Mesquita, L. M.; Strieder, M. M.; Contieri, L. S.; Pizani, R. S.; Sanches, V. L.; Viganó, J.; Bezerra, R. M. N.; Rostagno, M. A.; *Sustainable Chem. Pharm.* **2024**, *39*, 101558. [Crossref]
34. Shekaari, H.; Zafarani-Moattar, M. T.; Mokhtarpour, M.; Faraji, S.; *Sci. Rep.* **2023**, *13*, 11276. [Crossref]
35. García, A.; Rodríguez-Juan, E.; Rodríguez-Gutiérrez, G.; Rios, J. J.; Fernández-Bolaños, J.; *Food Chem.* **2016**, *197*, 554. [Crossref]
36. Nam, M. W; Zhao, J.; Lee, M. S.; Jeong, J. H.; Lee, J.; *Green Chem.* **2015**, *17*, 1718. [Crossref]
37. Khezeli, T.; Daneshfar, A.; *Ultrason. Sonochem.* **2017**, *38*, 590. [Crossref]
38. AlZahrani, Y. M.; Britton, M. M.; *Phys. Chem. Chem. Phys.* **2021**, *23*, 21913. [Crossref]
39. Zhou, P.; Zheng, M.; Li, X. Z.; Zhou, J.; Li, W. S.; Yang, Y. H.; *Int. J. Biol. Macromol.* **2023**, *242*, 125042. [Crossref]
40. Kamdem, M. C. M.; Fouegue, A. D. T.; Lai, N. J.; *Energies* **2023**, *16*, 3806. [Crossref]
41. Cai, C. Y.; Wang, Y. N.; Yu, W.; Wang, C. Y.; Li, F. F.; Tan, Z. J.; *J. Cleaner Prod.* **2020**, *274*, 123047. [Crossref]

*Submitted: April 20, 2024*
*Published online: August 28, 2024*